Impact of anoxia and oyster mortality on nutrient and microbial planktonic components: A mesocosm study

Julie Le Ray, Béatrice Bec, Annie Fiandrino, Franck Lagarde, Nicolas
Cimiterra, Patrick Raimbault, Cécile Roques, Sylvain Rigaud, Julie Régis,
Behzad Mostajir, et al.

Impact of anoxia and oyster mortality on nutrient and microbial planktonic components: A mesocosm study

Julie Le Ray [a,b,*], Béatrice Bec [b], Annie Fiandrino [c], Franck Lagarde [a], Nicolas Cimiterra [a], Patrick Raimbault [d], Cécile Roques [b], Sylvain Rigaud [e], Julie Régis [e], Behzad Mostajir [b], Sébastien Mas [f], Marion Richard [a]

[a] MARBEC, Univ Montpellier, CNRS, IRD, Ifremer, S`ete, France
[b] MARBEC, Univ Montpellier, CNRS, IRD, Ifremer, Montpellier, France
[c] MARBEC, Univ Montpellier, CNRS, IRD, Ifremer, La Seyne/mer, France
[d] Aix Marseille Univ., Université de Toulon, CNRS, IRD, MIO, Marseille, France
[e] Univ. Nîmes, EA 7352 CHROME, Rue Du Dr Georges Salan, F-30021 Nîmes, France
[f] MEDIMEER (Mediterranean platform for Marine Ecosystems Experimental Research), Observatoire de Recherche Méditerranéen de l'Environnement, Univ Montpellier, CNRS, IRD, INRAE, S`ete, France

ABSTRACT

The Thau lagoon is a Mediterranean coastal lagoon used for shellfish farming. It is periodically affected by anoxia events that trigger oyster mortality. To investigate the effects of an anoxia event focussed on nutrient dynamics and the responses of the microbial planktonic communities a 13-day in situ experiment was performed in September 2020. Transparent mesocosms (270 L) were placed at a depth of 4 m, inserted in the sediment, and kept closed throughout the experiment. The experiment comprised three treatments: i) Natural environment (N),
i.e. in the natural water outside the mesocosms containing a rope of 30 oysters (*Crassostrea gigas*), ii) Control mesocosm (C) filled with natural water with no oysters, and iii) Oyster mesocosm (O) filled with natural water containing a rope of 30 oysters. Oyster respiration in the oyster mesocosm depleted oxygen after 54 h. All the oysters from O mesocosm were dead after nine days and decomposition of their flesh combined with releases
from the water-sediment interface increased dissolved inorganic nitrogen (dominated by ammonium), phosphates, and ΣH_2S up to 390, 17 and 295 $\mu mol \cdot L^{-1}$, respectively. Phytoplankton biomass consequently increased by 20 (11.8 μg chl*al* $^{-1}$) and abundance by 4.5 (186×10^6 cells$\cdot L^1$) dominated largely by green algae <5 μm.
During the oyster mortality period (day 6 to day 9) high abundances of heterotrophic flagellates and large ciliate specimens were observed. This shift in the community towards small phytoplankton favours the microbial loop and is detrimental to shellfish farming. In a context of global warming in which the risk of anoxia is higher, the results of the present investigation demonstrate that anoxia triggers shellfish mortality and that the change in the plankton community disrupts the normal functioning of the ecosystem, causing serious financial losses. In this context, it is crucial to predict possible hypoxia and anoxia events using high frequency measurements of dissolved oxygen, by avoiding using shallow zones for oyster production and by reducing shellfish stocks, or by mechanically lifting the oysters out of the water during the night to reduce oxygen respiration in the ecosystem.

1. Introduction

Anoxia, defined as oxygen-depleted waters, and hypoxia, when concentrations are < 2 mg $O_2 \cdot L^{-1}$ (Diaz and Rosenberg, 2008) affect >500 sites in coastal waters worldwide (Breitburg et al., 2018). The loss of oxygen in these ecosystems has been partially attributed to climate warming. Indeed, rising temperatures reduce oxygen solubility in water and increase the stratification of water masses, thereby preventing vertical mixing (Schmidtko et al., 2017). Warming also affects living organisms by increasing their metabolic rates, consequently also increasing their oxygen uptake (respiration – Pernet et al., 2007; Pack et al., 2021). Coastal ecosystems are therefore particularly affected because they are highly productive, and their communities can significantly influence the concentrations of oxygen in the system (Pörtner, 2001). These ecosystems are closely linked to their watershed, a strong potential source of nutrients that promote growth. These ecosystems are shallow, meaning they are closely linked to the sediment, which requires oxygen for mineralisation, and is also a source of nutrients and a support for the attachment of macroalgae and seagrasses (Boynton et al., 1996). In coastal waters, anoxia has long been associated with eutrophication (Gooday et al., 2009), whether in lakes (Antoniades et al., 2011), bays (Zimmerman and Canuel, 2000), estuaries (D'Avanzo and Kremer, 1994) or lagoons (Newton et al., 2003).

Coastal lagoons are transitional waters located at the continent-ocean interface, partially confined (Guelorget et al., 1994; Fiandrino et al., 2017). These ecosystems are therefore particularly sensitive to anthropogenic pressures (Derolez et al., 2020a) as well as hydro-climatic conditions (Lagarde et al., 2021). The Thau lagoon is the largest, deepest and main shellfish production site along the French Mediterranean coast, and accounts for 10% of French oyster production (Gangnery et al., 2001).

In the past, the Thau lagoon was regularly affected by periods of anoxia in summer (Souchu et al., 1998; Harzallah and Chapelle, 2002; Hamon et al., 2003). The four main triggers of anoxic episodes are high air temperatures, high eutrophication rates, low winds and high precipitation (Derolez et al., 2020b). Following the improvement of wastewater treatment systems, the reduction in anthropic nutrient inputs reduced nitrogen and phosphorus concentrations and phytoplankton biomass (Derolez et al., 2020a). Combined with the reduction of rainfall and natural nutrient imports, this reduced the risk of eutrophication-related anoxia, resulting in a decade with no dystrophic crisis (Derolez et al., 2020b). However, with global warming, the risk of climate-induced anoxia has increased 3 fold for +1 °C. Anoxia is again observed in the lagoon, where the last dystrophic crisis, which occurred in 2018, was the result of high nutrient inputs combined with exceptional precipitation and a summer heatwave with very low winds (Lagarde et al., 2021).

The consequences of these dystrophic anoxic events are high concentrations of nutrients (ammonium, phosphates, silicates, and hydrogen sulphide) released from the sediment (Balzer et al., 1983; van der Loeff et al., 1984; Souchu et al., 1998). In the Thau lagoon, the anoxic zone can then spread to shellfish farming areas and lead to high shellfish mortalities on the farms, (2703 tons of oysters were lost in 2018 – Direction Départementale des Territoires et de la Mer de l'Hérault) along with releases of ammonium and phosphate, as already recorded during shellfish mortality events (Lomstein et al., 2006; Richard et al., 2019). These high nutrient concentrations resulted in blooms of diatoms (*Cylindrotheca* spp.) which were observed by the monitoring network (Lagarde et al., 2021). Diatom blooms are a response to the release of silicates at the water-sediment interface as observed during anoxia (Balzer et al., 1983; van der Loeff et al., 1984; Souchu et al., 1998).

The triggers of dystrophic crises and their impacts on shellfish stocks have been widely studied and modelled (Chapelle et al., 2000; Harzallah and Chapelle, 2002). Data are also available on nutrients in anoxic periods (Souchu et al., 1998). However, the ecological consequences for the microbial components in the environment, which support shellfish production, have not yet been observed, meaning the effects of anoxia on the microbial loop have not yet been described. In this context of increasing risks, the objective of this study was to determine the effects of

anoxia on nutrients and microbial components in a lagoon used for oyster farming. We conducted an in-situ experiment to reproduce anoxia in the presence or absence of oysters using mesocosms to test three hypotheses: (1) oxygen demand will be higher in presence of oysters and near the benthos; (2) nutrient concentrations will strongly increase during anoxia; (3) anoxia and associated oyster mortality will cause a shift in microbial planktonic communities.

2. Materials and methods

2.1. Study site

Thau lagoon is located on the French Mediterranean coast, it covers 67.9 km² and has an average depth of 4 m (Fiandrino et al., 2017). Pacific oysters (*Crassostrea gigas*) are reared on ropes suspended from metal structures, called "tables" (Gangnery et al., 2003). These structures account for 18% of the total surface area of the lagoon (Souchu et al., 2001).

2.2. Experimental design

Our in-situ study in the Thau lagoon lasted 13 days, from the 9th to the 22nd September 2020. Two mesocosms were submerged at a depth of 4 m in the lagoon and were inserted in the sediment under an experimental shellfish farm table (43°22′44.87″N, 3°34′37.64′E – Fig. 1) by scuba divers. The mesocosms were composed of a tube (length 2 m, diameter 40 cm) and a cylindrical base with the same diameter, 15 cm in height (Fig. 2), representing a total volume of 270 L. The principle of the experiment was to artificially reproduce the anoxic conditions caused by asphyxia due to the confinement of the water mass and organism respiration (van der Loeff et al., 1984) in presence or in absence of oysters. The experimental design comprised three treatments: **N**: the natural environment with a rope of 30 oysters, **C**: a control mesocosm containing only water, and **O**: a mesocosm containing water and a rope of 30 oysters (Fig. 2). The Pacific oysters used for the experiment came from a Thau shellfish farmer. The oysters used in the N and O treatments were on average 95.9 ± 9.9 mm in size and their average weight was 83.7 ± 17.5 g. This represented a total weight per treatment of 2.5 ± 0.5 kg, corresponding to 285.5 ± 83.5 g of oyster flesh inside the mesocosm, which is within the range used by farmers. Two sampling depths were used for each treatment: P for Pelagic layer (ca. 130 cm above the sediment) and B for Benthic layer (ca. 30 cm above the sediment: Fig. 2). Syringes (450 mL), equipped with the Luer Lock system, were used to sample the water around 10 and 11 am on days: 0, 1, 2, 6, 9 and 13. Considering, the importance of light intensity, sampling was made as quickly as possible, at similar hours on each day and in the morning to ensure water conditioning during working hours. Three replicate samples were collected for each treatment and the two depths. A tap located at the top of the mesocosm was switched on during sampling to avoid changing the volume of water in the mesocosms and/or the sucking porewater. The tap was equipped with online 20 and 5 μm filters to avoid contaminating the mesocosm with environmental microbes. At the surface, the syringes were plugged with caps to avoid exchanges
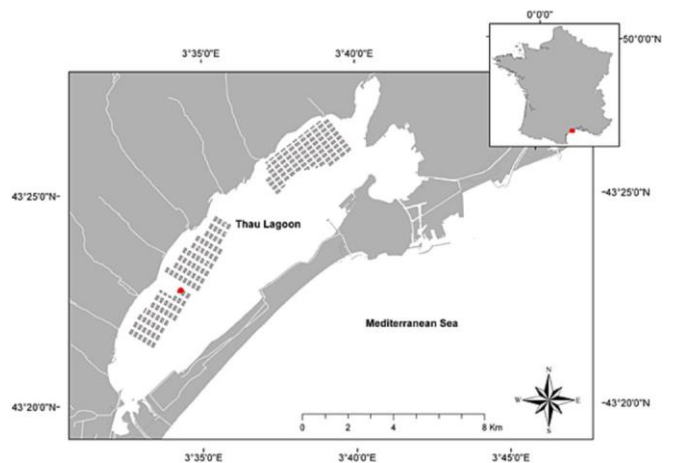

Fig. 1. Location of the Thau lagoon and of the experimental table where the mesocosms were set up.
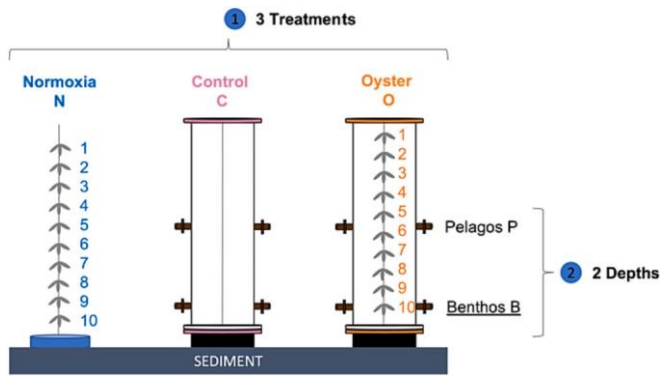
Fig. 2. Schematic diagram of the experimental design comprised of three treatments (N: Natural environment, C: Control and O; Oyster), 2 depths (P: Pelagic layer and B: Benthic layer), and 6 sampling dates (0, 1, 2, 6, 9, 13 days). The samples taken at the two depths were replicated 3 times on each sampling date for each treatment.

with the air. The syringes were transported to the lab in coolers. In the laboratory, the water was processed within 4 h of after sampling, depending on the parameter to be studied. To determine the mortality rate of the oysters, the status of the oyster underwater (open, closed or dead) was observed by the same scuba diver in all treatments on each sampling occasion. These observations were made before starting to sample the water to avoid stressing the oysters. At the same time, the scuba diver recorded the colour of the water and took photographs using a GoPro Hero 4 camera.

2.3. Sample conservation and analysis

2.3.1. Salinity, pressure, temperature, and dissolved oxygen

Autonomous probes were used to continuously monitor salinity (HOBO U24 U24–002-C), and barometric pressure (HOBO U20L-4) on site throughout the experiment. Temperature, and oxygen (HOBO U26–001) were measured at 30-min intervals at both depths in each treatment. The oxygen measurements were then corrected with pressure and salinity using HOBOware Pro software.

2.3.2. Chemical parameters

To preserve the nutrient samples (ammonium, nitrate, nitrite and phosphate), 90 mL of water were filtered through a GF/F Whatman filter (0.7 μm pore size) before being stored at —20 °C. For silicates, 40 mL of sample were filtered on Whatman syringe filters (*cellulose* membrane 0.2 μm pore size), then stored at 4 °C. For hydrogen sulphide ($\sum H_2S$), 0.5 mL of water previously filtered on a cellulose acetate membrane 0.22 μm pore size were placed in an Eppendorf tube containing 1.5 mL of zinc acetate and analyses were performed by spectrophotometry (DR2800 Hach Lange) using the methylene blue method (Cline, 1969). Concentrations of nitrite (NO_2^-), nitrate (NO_3^-), orthophosphate (PO_4^{3-}) and silicate ($Si(OH)_4$) were measured by automated colorimetry according to the protocol of Aminot et al. (2007). Detection limits were 0.05 μmol·L^{-1} for nitrite, nitrate, and phosphate, and 0.1 μmol·L^{-1} for silicate. To ensure the reproducibility of nutrient measurements between analyses, in-house standards were first compared to available certified OSIL references. Ammonium concentrations were measured using the sensitive method of Holmes et al. (1999) with a detection limit of 5 nmol·L^{-1}.

2.3.3. Biological parameters

Cytometry samples (virus, heterotrophic prokaryotes and phytoplankton <20 μm, 1 mL) were fixed with glutaraldehyde (0.5% final concentration). After 15 min at 4 °C in the dark, the samples were flash frozen in liquid nitrogen and then stored at —80 °C until analysis.

Virus samples were stained with SYBR green I for 10 min in the dark at 80 °C to allow the stain to penetrate the capsid. Virus abundances (mL^{-1}) were then estimated with a FacsCanto II cytometer following (Brussaard, 2004).

For abundances of heterotrophic prokaryotes (including heterotrophic bacteria and archaea), the samples were marked with SYBR green I (Molecular probes) for 15 min at 4 °C in the dark according to (Marie et al., 1997). Abundances were determined by flow cytometry using a Cytoflex Beckman Coulter, at a speed of 20 μL·min^{-1}. Fluorescent beads were added to the sample as size references (1 and 2 μm, Polysciences). To calculate the volume analysed, a known amount of BD Trucount™ beads was used. The total abundances of bacteria (cells·mL^{-1}) were estimated based on their forward scatter (FSC) and their fluorescence level was estimated using FL1 dye (fluorescent channel 525/40 BP).

Total and size-fractionated chlorophyll *a* (chl*a*) biomass were estimated using whole water (total chl*a*), and prefiltered water on a 20-μm pore-size membrane (<20 μm chl*a*) and on a membrane 5 μm pore size (<5 μm chl*a*). Size-fractionated biomass determined using Nuclepore membranes (5 and 20 μm pore size) allowed us to determine chl*a* for different size classes: microphytoplankton (>20 μm), nanophytoplankton (5–20 μm) and ultraphytoplankton (<5 μm). For each sample, 100 mL of prefiltered or whole water was filtered on a Whatman GF/F membrane (0.7 μm pore size). The filters were then stored at —20 °C until analysis. The pigments were extracted in 90% acetone by grinding the filter stored in tubes. Pigments from the ground filters were extracted in the dark for 24 h at 4 °C. The samples were then centrifuged at 4800 rpm for 20 min, the supernatant was collected to measure chlorophylls (chl *a*, *b* and *c*, μg·L^{-1}) using fluorescence spectroscopy (Perkin-Elmer LS50b) and calculated according to (Neveux and Lantoine, 1993). Chl*a* is a proxy of phytoplankton biomass, chl*b* of green algae, and chl*c* of golden-brown algae.

To assess abundances of pico- and nanophytoplankton (<20 μm), cells were counted with a Cytoflex Beckman Coulter at two laser excitation wavelengths (488 and 638 nm). These wavelengths enabled measurement of four types of fluorescence: FL1 (525/40 BP), FL2 (585/42 nm - phycoerythrin), FL4 (690/50 nm - chl*a*) and FL6 (660/10 nm - phycocyanin). Fluorescent beads were added to the samples as size references (Polysciences - 1, 2, 3, 6 and 10 μm). The relative size of the enumerated cells was estimated from their FSC level and the position of the fluorescent beads on the cytogram. Acquisition was at a speed of 36 μL.min^{-1}. To determine the exact volume analysed, a known amount of BD Trucount™ beads were used. Cytograms were visualised and treatment was performed using CytExpert software. We distinguished between populations as a function of their relative size (FSC) and their fluorescence. Picocyanobacteria (<1 μm) were identified by their orange fluorescence (FL2) for phycoerythrin-rich cyanobacterias and their red fluorescence (FL6) for phycocyanin-rich cyanobacterias. We identified autotrophic picoeukaryotes and nanophytoplankton by their red fluorescence due to Chl*a* (FL4) and their relative size (FSC). The two groups were separated according to their size: picophytoplankton (<3 μm) and nanophytoplankton (>3 μm).

Following a decantation step of 12 h in the dark, phytoplankton >20 μm were identified using an Olympus IMT2 inverted light microscope as described by (Utermöhl, 1958).

Protist abundances were only measured in the Pelagic samples and on days 0, 6, 9 and 13. To evaluate the abundances of flagellates (cells·L^{-1}), on days 0, 6, 9 and 13, 30 mL of water were fixed with formaldehyde at a final concentration of 4% and stored at 4 °C. On the same days, water was fixed with lugol at a final concentration of 2% to measure ciliate abundances (cells·L^{-1}).

To count heterotrophic flagellates (HF) and autotrophic flagellates (AF), the DNA inside the samples was marked with 4′,6-diamidino-2-phenylindole (DAPI) and filtered on black nucleopore polycarbonate filters (0.2 μm pore size), as described in (Vidussi et al., 2011). An epifluorescence microscope (Olympus AX-70, magnification x1000) with UV excitation was used for counting. The DNA showed blue fluorescence and the chl*a* showed red fluorescence. Thus, to differentiate between the

two types of flagellates, organisms showing double fluorescence were considered autotrophs, while organisms only showing blue fluorescence were considered heterotrophs. Each organism counted was then assigned to a size class of <5, 5–10, 10–20, and > 20 μm. Following 24 h of sedimentation in a Ütermöhl settling chamber, the ciliate populations were counted using an Olympus IX-70 inverted microscope, as described in (Vidussi et al., 2011). Each organism counted was sorted by size (< 12.5 μm, 12.5–25 μm, 25–50 μm and > 50 μm), and, when possible, by taxonomy (up to genus level).

2.4. Statistical analyses

Figures and statistical analyses were performed with R software version 4.1.2. Results were analysed using repeated-measures ANOVAs with an autocorrelation structure in the model for temporal series, using the function gls in the Rcompanion package. Two models were calculated. For the first model, treatments were considered as random variables. The first model was then compared to the second one that was a model with no treatment effect. This made it possible to detect the effect of the treatment. Additional repeated measures ANOVAs with autocorrelation were then performed to test the effects of time and depth and their interaction in each treatment, separately (Supplementary materials – Tables 1 to 3). A principal component analysis (PCA) was also performed to show the effect of the treatment and depth of the experiment using the Factoshiny package. A p-value was considered significant at <0.05.

3. Results

3.1. Evolution of salinity, temperature, and dissolved oxygen

Salinity averaged 40.5 ± 0.1 over the study period. In all treatments, temperatures varied over the course of the experiment with lower temperatures recorded at night and higher temperatures during the day. Temperatures varied between treatments (Table 1), with higher values in the N treatment than in the C and O treatments (Supplementary materials – Fig. 1). In the N treatment, the temperature increased with time from 22.4 to 25.3 °C with higher temperatures in the Pelagic layer than in the Benthic layer. Inside the mesocosms (C and O treatments, with no significant difference), the temperature varied in the same way as in the N treatment. The temperature increased by 2.4 °C from 22.5 °C

(in the Benthic layer in the C and O treatments on day 0) to 24.9 °C (in the Pelagic layer in C and O on day 9).

Oxygen recording started at 2:30:00 pm on the 9th of September 2020, when the initial values were 6.3 ± 0.6 mg·L⁻¹. An effect of treatment was demonstrated for oxygen using repeated measures ANOVAs (Table 1), with higher values in N, followed by C, and the lowest in the O treatment (Fig. 3). Considering the three treatments together, oxygen varied according to depth and day interactions (Supplementary materials – Tables 1 to 3). In the N treatment, a bigger difference between the two depths was observed at the beginning of the experiment, with higher means in the Pelagic layer. Over the course of the experiment, mean oxygen was 6.37 ± 0.68 in the Pelagic layer vs. 6.10 ± 1.07 mg.L⁻¹ in the Benthic layer, with a minimum of 2.38 mg. L⁻¹ measured in the Benthic layer at 5:30 am on day 2) and a maximum of 9.71 mg.L⁻¹ measured in the Pelagic layer at 1:30 pm on day 7. In the C treatment, a decrease in oxygen was recorded over time resulting in higher values in the Pelagic layer than in the Benthic one at the end of the experiment. Mean oxygen in the Pelagic layer was 5.96 ± 0.74 while mean oxygen in the Benthic layer was 4.34 ± 0.88 mg·L⁻¹, with a minimum of 1.32 mg·L⁻¹ measured in the Benthic layer under hypoxic conditions at 11:30 pm on day 11 and a maximum of 6.91 mg·L⁻¹ measured in the Pelagic layer at 8:30 pm on day 0. Variations in nychthemeral values were observed in the N and C treatments, with higher values recorded during the day. In the O treatment, the maximum concentration was 6.16 mg·L⁻¹ recorded at 2:30 pm on day 0 in the Pelagic layer. The oxygen concentrations then rapidly decreased to reach 0.00 mg·L⁻¹, i.e., anoxia. This state was reached in the Pelagic layer after 52 h and in the Benthic layer, two hours later (i.e. 54 h) and remained stable throughout the experiment.

3.2. Oyster mortality and water colour observations

No oyster mortality was observed in the N treatment. In the O treatment, on day 6, oysters were 100% open in contrast to in the N treatment (Fig. 4A). All the oysters in the O treatment died between day 6 and day 9. At the end of the experiment, all oyster flesh was fully decomposed and only the shells remained attached to the ropes. What is more, in the O treatment, the colour of the water changed from clear on day 0 (Fig. 4A), to green on day 6 (Fig. 4B), and was whitish from day 9 on (Fig. 4C). At the end of the experiment, the walls of the O mesocosm were covered with microalgae.

3.3. Temporal variability of nutrients

A significant effect of the treatment was detected for all nutrients (Table 1), with higher values in the O treatment than in the C or N treatments. Within each treatment, the nutrients varied significantly
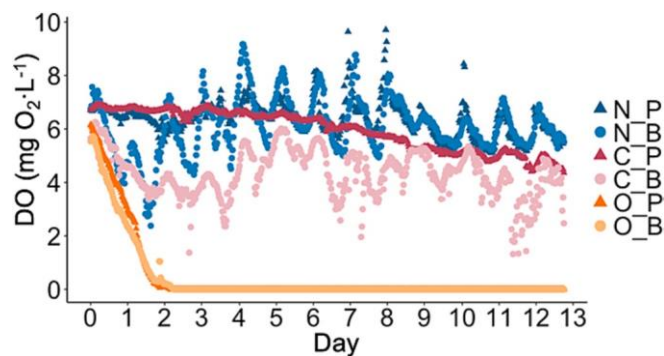
Table 1

Results of repeated-measures ANOVAs testing the effect of treatment (C, N vs. O), with temporal autocorrelation. p-values <0.05 are in **bold**.

Parameter	Auto-correlation	model vs model.fixed	
Temperature	0.92	**<0.0001**	***
Oxygen	0.99	**<0.0001**	***
DIN	0.75	**<0.0001**	***
Phosphates	0.77	**<0.0001**	***
Silicates	0.73	**<0.0001**	***
Hydrogen sulphide	0.78	**<0.0001**	***
Viruses	0.25	**0.0016**	**
Bacteria	0.76	**<0.0001**	***
Total chlorophyll *a*	0.76	**<0.0001**	***
<5 μm	0.77	**<0.0001**	***
5-20 μm	0.63	**0.0025**	**
>20 μm	0.58	0.0626	
Picocyanobacteria abundances	0.79	**<0.0001**	***
Picoeukaryotes abundances	0.74	**<0.0001**	***
Nanophytoplankton abundances	0.72	**<0.0001**	***
Heterotrophic flagellates	0.54	**0.0044**	**
Autotrophic flagellates	0.58	**<0.0001**	***
Total ciliate abundances	0.44	0.3714	
<12.5 μm	0.07	0.6412	
12.5-25 μm	0.21	0.4591	
25-50 μm	0.54	0.1154	
>50 μm	0.51	0.4830	

Fig. 3. Oxygen concentrations (mg·L⁻¹) measured at 30-min intervals for each treatment (N: Natural environment, C: Control (Mesocosm with no oysters), O: Oyster (Mesocosm with oysters)) at the two depths (P: Pelagic layer, B: Benthic layer) during the 13-day experiment (September 2020, Thau lagoon, France).
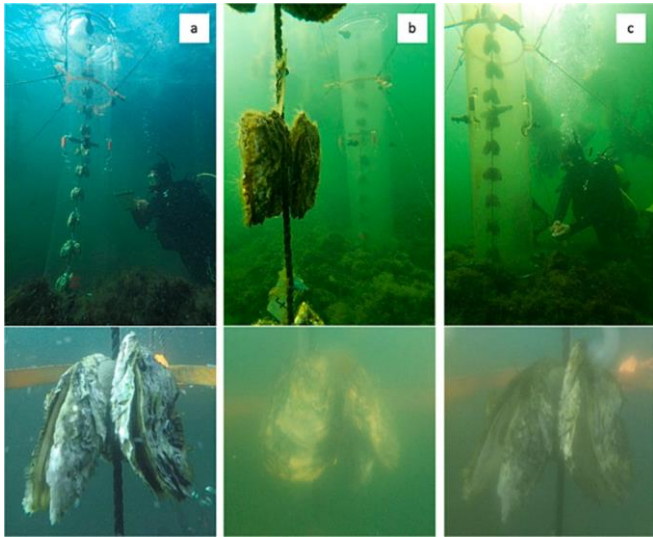
Fig. 4. Photos of changes in the mesocosm O and its oysters, on A) 15 September 2020 corresponding to day 6, B) 18 September 2020 corresponding to day 9 and C) 22 September 2020 corresponding to day 13.

depending on day and depth interactions (Supplementary materials – Tables 1 to 3).

In all three treatments, the main form of dissolved inorganic nitrogen (DIN) was NH_4^+, ranging from a minimum 76.7% in the Pelagic layer in the C treatment to a maximum of 99.8% in the Benthic layer in the O treatment. Initial DIN values in all treatments (Fig. 5A) were 0.81 ± 0.24 µmol·L^{-1}. In the N treatment, means remained low (P: 0.66 ± 0.22 vs. B: 0.95 ± 0.12 µmol.L^{-1}). The difference between the Pelagic and Benthic layer reached maximum on day 9 with the lowest value (0.29 ± 0.01 µmol·L^{-1}) measured in the Pelagic layer. In the C treatment (Fig. 5A), a significant difference was observed between the Pelagic and Benthic layers. NID was maximum on day 2 with a value of 5.02 ± 0.11 in the Benthic layer and 0.22 ± 0.02 µmol·L^{-1} in the Pelagic layer. In the Benthic layer, this corresponded to an increase by a factor of 5 until day 2 after which NID decreased by a factor of 8 to reach 0.65 ± 0.05 µmol. L^{-1} on day 13, the last day of the experiment. In the O treatment (Fig. 5B), concentrations of NID increased by a factor of 580 in the Pelagic layer and by a factor of 535 in the Benthic layer until day 9 (P: 388.7 ± 0.7 and B: 358.9 ± 13.7 µmol·L^{-1}). Concentrations then decreased by a factor of 3.5 and 3.3 respectively to reach a mean of 111.4 ± 2.2 µmol.L^{-1}, at both depths.

Initial phosphates values were 0.15 ± 0.05 µmol·L^{-1} (Fig. 5C). In the N treatment, the mean phosphate decreased by a factor of 2.5 from day 2
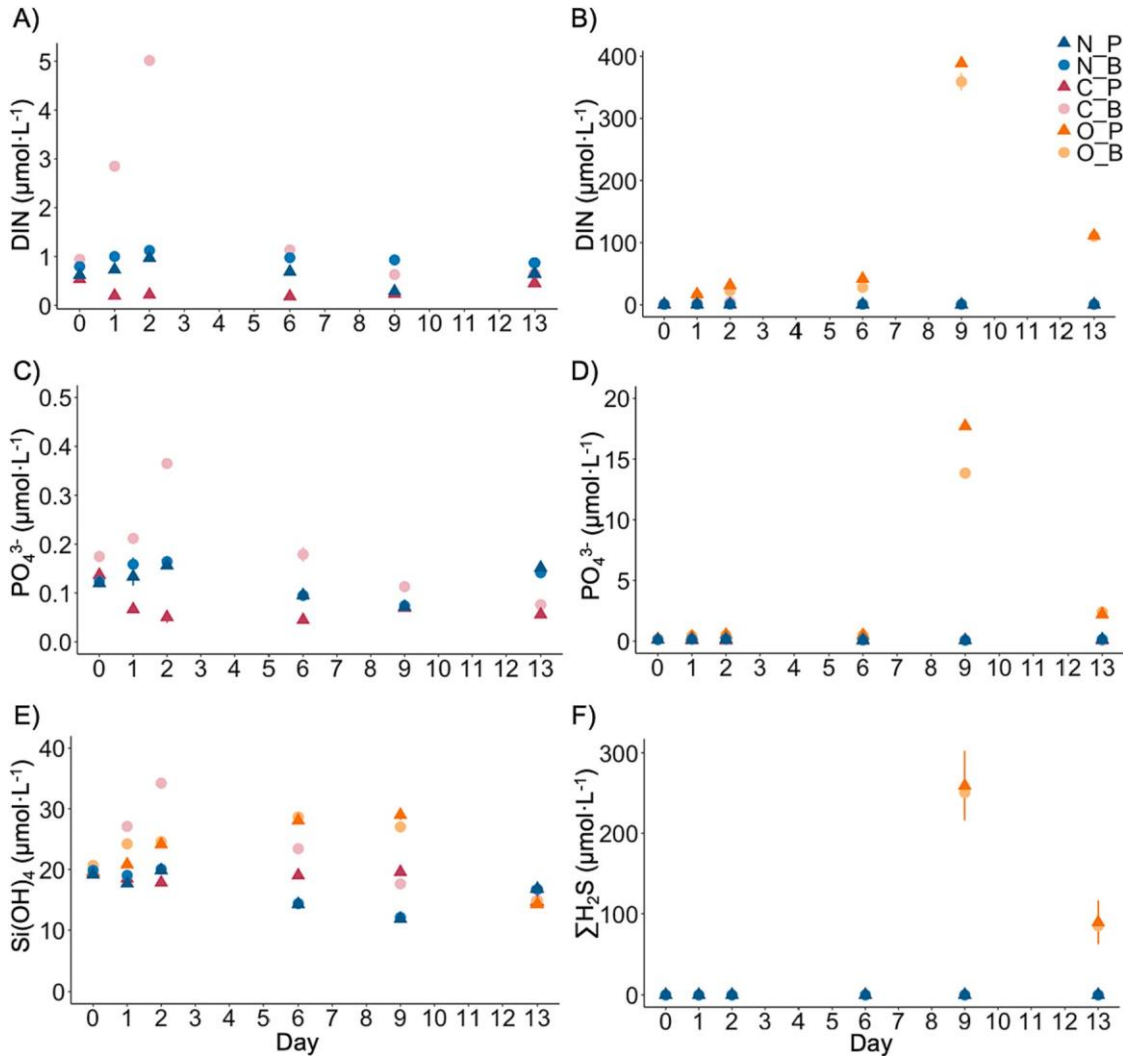

Fig. 5. Mean concentrations (±SD) of (A) DIN in the N and C treatments, (B) DIN in all treatments, (C) PO_4^{3-} in the N and C treatments, (D) PO_4^{3-} in all treatments, (E) $Si(OH)_4$ and (F) H_2S observed for each treatment separately, (N: Natural environment, C: Control (Mesocosm with no oysters), O: Oyster (Mesocosm with oysters)) and the two depths (P: Pelagic layer, B: Benthic layer) on days 0, 1, 2, 6, 9 and 13 (September 2020, Thau lagoon, France).

until day 9 in both the Pelagic and Benthic layers and then increased by a factor of 2.1 until day 13 (Fig. 5C). However, at both depths, the values remained very low with an average of 0.12 ± 0.03 μmol·L⁻¹ throughout the experiment. In the C treatment (Fig. 5C), the dynamics differed between depths. In the Pelagic layer, concentrations decreased by a factor of 3.5 between day 0 and day 2. No significant difference was observed from day 6 to day 13, with concentrations remaining around 0.06 ± 0.01 μmol·L⁻¹. In the Benthic layer, concentrations increased by a factor of 2.1 to reach maximum (0.37 ± 0.01 μmol·L⁻¹) on day 2 and then decreased by a factor of 5.3 until day 13, to reach a value of 0.08 ± 0.01 μmol·L⁻¹ (Fig. 5C). In the O treatment (Fig. 5D), concentrations increased by a factor of 137 in the Pelagic layer and by a factor of 108 in the Benthic layer until day 9, and reached 17.72 ± 0.21 and 13.84 ± 0.29 μmol·L⁻¹ respectively. Concentrations then decreased by a factor of 8.1 in the Pelagic layer and by a factor of 5.8 in the Benthic layer, to reach 0.17 ± 0.08 μmol.L⁻¹ at both depths.

Mean silicate concentrations (Fig. 5E) decreased in the N treatment from the beginning of the experiment until day 9, by a factor of 1.69 in the Pelagic layer and by a factor of 1.67 in the Benthic layer, then increased by a factor of 1.2 until day 13 at both depths. The mean values for the whole experiment were 16.62 ± 2.85 μmol·L⁻¹ in the Pelagic layer and 17.02 ± 3.05 μmol·L⁻¹ in the Benthic layer. In the C treatment, the highest mean value was measured in the Benthic layer on day 2 when the maximum difference between depths was detected (Benthic: 34.22 ± 0.62 vs. Pelagic: 17.84 ± 0.10 μmol.L⁻¹). The concentrations then decreased by a factor of 1.35 in the Pelagic layer and by a factor of 2.36 in the Benthic layer to reach 14.80 ± 0.14 μmol·L⁻¹ at both depths. In the O treatment (Fig. 5C), a 1.4 fold increase was observed until day 9, to reach 29.00 ± 0.84 in the Pelagic layer and 27.02 ± 0.13 μmol·L⁻¹ in the Benthic layer. The concentrations then decreased by a factor of 2.1 in the Pelagic layer and by a factor of 2.0 in the Benthic layer to reach 14.5 ± 0.3 μmol·L-1 in both layers.

Hydrogen sulphide (Fig. 5F) was only detected in the oyster mesocosm (O treatment) with no differences between depths (Supplementary materials – Table 3). Hydrogen sulphide concentrations only became significant between day 9 (254.9 ± 33.2 μmol·L-1) and day 13 (87 ± 18 μmol.L-1).

3.4. Virus and heterotrophic prokaryote abundances

Repeated-measures ANOVAs revealed a significant effect of treatment on virus abundances (Table 1), with higher values in the O treatment than in the N and C treatments (Supplementary materials – Fig. 2). Initial virus abundances were 26.6 ± 5.4 × 10⁶ mL⁻¹. In the N and the C treatment, no significant effect of the depth or day was detected (Supplementary materials – Tables 1 and 2), the mean abundances over the 13-day experiment were 30.0 ± 5.1 × 10⁶ mL⁻¹ for the N treatment and 26.3 ± 4.6 × 10⁶ mL⁻¹ for the C treatment. In the O treatment, the interaction between day and depth was significant (Supplementary materials – Table 3) with higher abundances in the Benthic layer than in the Pelagic layer at the end of the experiment (45.2 ± 6.7 × 10⁶ and 37.1 ± 8.2 × 10⁶ mL⁻¹ respectively).

An effect of treatment on the abundances of heterotrophic prokaryotes was detected (H. Prokaryotes - Table 1). Initial abundances were 2.7 ± 0.3 × 10⁶ cells·mL⁻¹. In the N treatment, abundances varied significantly depending on the day and depth (Supplementary materials – Table 1) the highest means being observed in the Pelagic layer rather than in the Benthic layer, except on day 6. The same temporal dynamics was observed at the two depths: the mean increased from day 0 to day 6 to reach a value of 3.4 ± 0.3 × 10⁶ cells·mL⁻¹ maintained between day 6 and day 13 (Fig. 6). In the C treatment (Supplementary materials – Table 2), an effect of interaction between day and depth was observed on H. Prokaryotes. Abundances fluctuated slightly around 2.7 ± 0.4 × 10⁶ cells·mL⁻¹, except in the Pelagic layer on day 1, when the value was higher (3.4 ± 0.2 × 10⁶ cells·mL⁻¹). In the O treatment (Supplementary materials – Table 3), depth was a significant factor of variation for H.
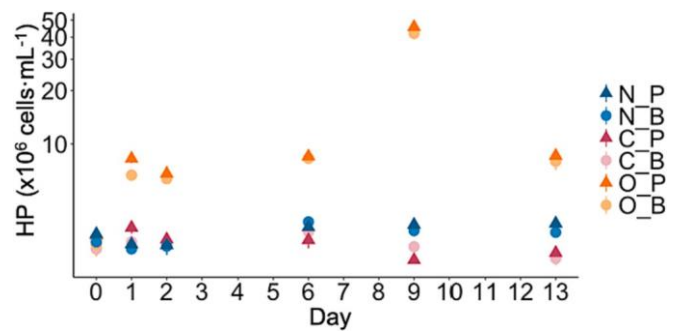

Fig. 6. Mean abundances (±SD) of H. Prokaryotes with a logarithmic scale in all treatments (N: Natural environment, C: Control (Mesocosm with no oysters), O: Oyster (Mesocosm with oysters)) and depth (P: Pelagic layer, B: Benthic layer) on days 0, 1, 2, 6, 9 and 13 (September 2020, Thau lagoon, France).

Prokaryotes, with higher abundances observed in the Pelagic layer than in the Benthic layer, whatever the day. There was also a day effect with a strong increase by a factor of 16 from day 0 to day 9 (45.7 ± 1.1 × 10⁶ in the Pelagic layer and 42.0 ± 3.1 × 10⁶ cells·mL⁻¹ in the Benthic layer). Abundances then decreased until the end of the experiment (by a factor of 5.5 in the Pelagic layer and by a factor of 5.7 in the Benthic layer - Fig. 6).

3.5. Evolution of the phytoplanktonic community

Total chlorophyll *a* (chl*a*.TOT) biomass varied significantly between treatments (Table 1), with higher values in the O treatment than in the C treatment and even higher than in the N treatment. At the beginning of the experiment, mean chl*a*.TOT was 0.58 ± 0.13 μg·L⁻¹. Chl*a* biomasses of ultraphytoplankton (< 5 μm) and nanophytoplankton (5–20 μm) differed significantly between treatments, which was not the case for the microphytoplankton (> 20 μm, Table 1). In the N treatment, there was a day effect on chl*a*.TOT (Supplementary materials – Table 1), with a 2.1-fold increase in concentrations over time whatever the depth (mean at d13: 0.98 ± 0.14 μg·L⁻¹). In the N treatment, the slight increase in chl*a*. TOT was most often associated with a development of microphytoplankton over time representing a contribution of up to 63% for 0.74 μg·L⁻¹ on day 9 (Fig. 7A-B). In the C treatment (Supplementary materials – Table 2), chl*a*.TOT varied significantly at the two depths over the course of the experiment, with a peak in biomass (2.63 ± 0.63 μg·L⁻¹) in the Benthic layer reached on day 6. Considering the associated accessory pigments, this increase in phytoplankton biomass was associated with an increase in chl*c*, and in nanophytoplankton (32%) and microphytoplankton (57%). In the Pelagic layer, the concentrations increased less than in the Benthic layer over the course of the experiment and reached a final value of 1.32 ± 0.27 μg·L⁻¹ (Fig. 7D). In the O treatment, (Supplementary materials – Table 3), chl*a*.TOT varied with the day and depth interaction. A marked increase was observed during the first nine days at both depths with a maximum of 11.69 ± 0.26 μg·L⁻¹ in the Pelagic layer and 9.43 ± 0.31 μg·L⁻¹ in the Benthic layer (Fig. 7E-F) at day 9. This corresponded to an increase of a factor of 20.5 and 16.7, respectively. This increase in concentration was associated with a peak in chl*b*, dominated by ultraphytoplankton which increased to 71% in the Pelagic layer (8.3 μg·L⁻¹) and to 75% in the Benthic layer (7.1 μg·L⁻¹). The mean concentration of chl*a*.TOT then decreased to 3.63 ± 0.42 μg·L⁻¹.

Based on flow cytometric analyses, picophytoplankton was composed of phycoerythrin picocyanobacteria (CYANO), and four populations of picoeukaryotes (PEUK). The abundances of CYANO, PEUK and nanophytoplankton (NANO) varied significantly between treatments (Table 1). The initial mean values for CYANO, PEUK and NANO in all treatments were 4.5 ± 0.5 × 10⁶, 40.2 ± 8.8 × 10⁶, and 0.7 ± 0.2 × 10⁶ cells·L⁻¹, respectively. In the N treatment, CYANO
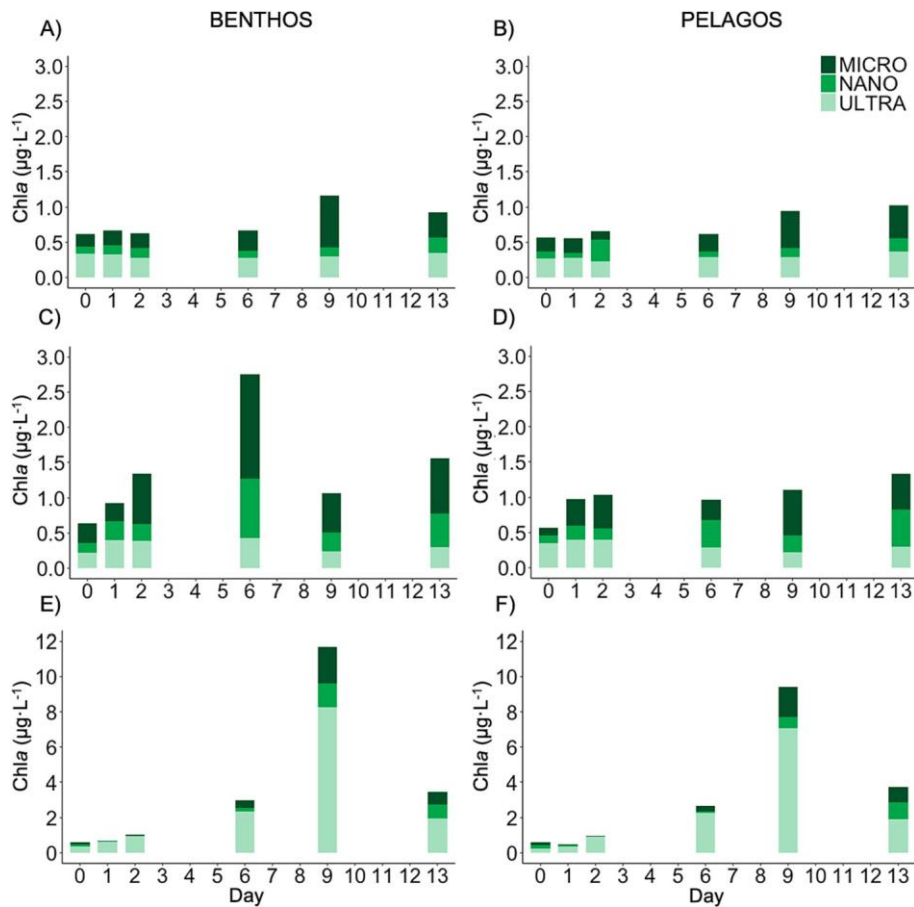
Fig. 7. Mean concentrations (±SD) of chl*a* and contribution of microphytoplankton, nanophytoplankton and ultraphytoplankton to the chlorophyll biomass observed in each treatment (N: Natural environment, C: Control (Mesocosm with no oysters), O: Oyster (Mesocosm with oysters)) and at the two depths (P: Pelagic layer, B: Benthic layer) on days 0, 1, 2, 6, 9 and 13 (September 2020, Thau lagoon, France).

abundances varied according to the day and depth but there was no influence of day/depth interactions (Supplementary materials – Table 1). Higher means were observed in the Pelagic layer than in the Benthic layer. The same dynamics was observed at both depths with an increase in concentration from day 2 to day 9 (Benthic layer: $64.3 \pm 2.1 \times 10^6$ cells·L^{-1}; Pelagic layer: $69.3 \pm 6.6 \times 10^6$ cells·L^{-1}), followed by a slight decrease until day 13. The abundances of PEUK and NANO varied according to depth and day interaction (Table 1). Picoeukaryotes had an average of $49.3 \pm 13.9 \times 10^6$ cells·L^{-1} in the Pelagic layer and $40.1 \pm 15.0 \times 10^6$ cells·L^{-1} in the Benthic layer. Nanophytoplankton abundances increased slightly over time to reach a peak on day 9. Mean abundances were 0.9 ± 0.3 in the Pelagic layer and $0.8 \pm 0.3 \times 10^6$ cells·L^{-1} in the Benthic layer. In the C treatment (Supplementary materials – Table 2), CYANO, PEUK and NANO varied according to the day and depth interactions. CYANO abundances increased until the last day (day 13) with similar abundances in the two layers on day 13 ($48.2 \pm 3.1 \times 10^6$ cells·L^{-1} - Fig. 8A). The abundances of PEUK oscillated over the course of the experiment with higher values in the Pelagic layer on day 1 and day 2 (day 1: 84.1×10^6 cells·L^{-1} - Fig. 8B). The abundances of nanophytoplankton increased over time with higher values in the Benthic layer on day 1, day 2 and day 6. The final values (day 13) were similar in the two layers with $2.2 \pm 0.1 \times 10^6$ cells·L^{-1} (Fig. 8C). In the O treatment (Supplementary materials – Table 3), all phytoplankton components varied with the day-depth interaction. Picocyanobacteria abundances increased over time but less than in the other treatments, and reached a final value of $27.3 \pm 1.4 \times 10^6$ cells·L^{-1}. Picoeukaryotes abundances varied depending on the day and reached a peak on day 9 with $202 \pm 5 \times 10^6$ cells·L^{-1} in the Pelagic layer and $169 \pm 8 \times 10^6$ cells·L^{-1} in the Benthic layer (Fig. 8B). This peak was associated with a

single population around 3–4 μm in size (PEUK 4). NANO abundances first decreased from day 0 to day 2 then increased from day 6 to day 9. The final NANO abundances on day 13 were lower than in the C treatment and higher than in the N treatment: $1.7 \pm 0.2 \times 10^6$ cells·L^{-1} in the Pelagic layer and $1.9 \pm 0.3 \times 10^6$ cells·L^{-1} in the Benthic layer.

For microphytoplankton species (>20 μm), microscopic observations enabled identification of the species present at the beginning and at the end of the experiment. At the beginning, the microphytoplankton in all treatments was dominated by one taxon, *Rhizosolenia setigera*. At the end of the N treatment, 10 taxa (only diatoms) were present with *Skeletonema* spp. dominating, while dinoflagellates were no longer detected. In the C treatment, eight taxa (diatoms and dinoflagellates) were present dominated by *Skeletonema* spp. like in the N treatment. In the O treatment, seven taxa were detected dominated by *Cylindrotheca* spp.

3.6. Evolution of grazing protists community

The size classes of autotrophic flagellates (AF) are not presented here because most organisms were in the 5–10 μm class, and the same trend was observed for heterotrophic flagellates (HF) of which 95% were in the <5 μm size-class. The treatment had a significant effect on protist abundances (Table 1). In the N treatment, the abundances of AF increased by 2.7 fold over the course of the experiment (from an initial concentration $0.62 \pm 0.23 \times 10^3$ cells·L^{-1} to a final concentration $1.62 \pm 0.02 \times 10^3$ cells·L^{-1}). In the C treatment, the abundance of AF decreased from day 0 to day 6 ($0.06 \pm 0.03 \times 10^3$ cells·L^{-1}), then increased until day 13. In the O treatment, AF were no longer detected after day 6. Abundances of HF in the N treatment did not change over time (Supplementary materials – Tables 1 to 3) the average being 2.26
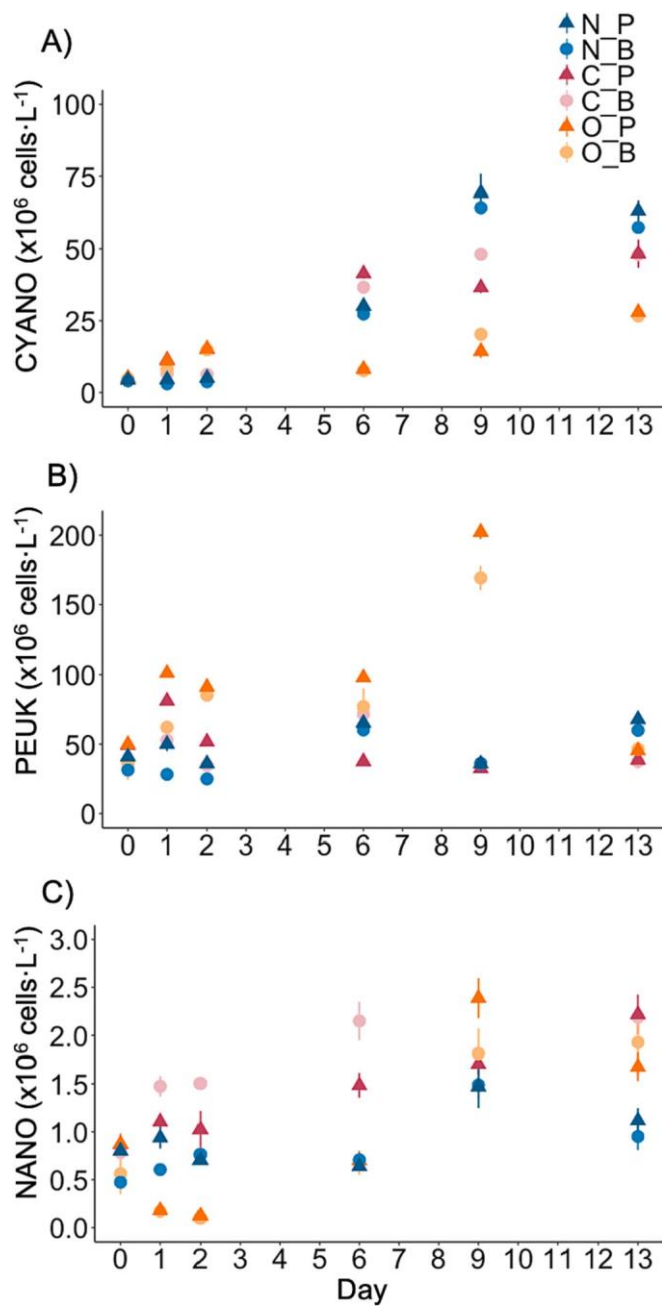
Fig. 8. Mean abundances (±SD) of <20 μm phytoplankton, (A) picocyano-bacteria (CYANO), (B) picoeukaryotes (PEUK), and (C) nanophytoplankton (NANO) observed in each treatment (N: Natural environment, C: Control (Mesocosm with no oysters), O: Oyster (Mesocosm with oysters)) and depth (P: Pelagic layer, B: Benthic layer) on days 0, 1, 2, 6, 9 and 13 (September 2020, Thau lagoon, France).

± 0.43 × 10³ cells·L⁻¹. In the C treatment, abundances increased over time from day 0 (2.32 ± 0.51 × 10³ cells·L⁻¹) to day 13 (4.67 ± 0.26 × 10³ cells·L⁻¹). In the O treatment, abundances increased sharply to reach a peak on day 9 (107.44 ± 9.1 × 10³ cells·L⁻¹), then decreased by 7 fold on day 13 (Supplementary materials – Fig. 3).

No effect of treatment was observed on the abundance of ciliates whatever their size fraction (Table 1). Initial values were 0.19 ± 0.10 × 10³ cells·L⁻¹ (Supplementary materials – Fig. 4). In the N treatment, ciliates increased by a factor of 13 until day 13 when they reached 3.46 ± 1.71 × 10³ cells.L⁻¹. All size classes were involved except 12.5–25 μm. This 19.2-fold increase was mostly associated with tintinnids (included

in the 25–50 μm size class) and to a lesser extent with *Mesodinium* sp. In the C treatment, abundances increased until day 6 but less than in the N treatment (1.04 ± 1.32 cells·L⁻¹). The peak on day 6 involved different ciliates (tintinnid, holotrich, *Strobilidium* sp. and *Strombidium* sp.). After day 6, abundances decreased sharply. Tintinnids were no longer detected in the C treatment. On day 13, *Strombidium* sp., *Strobilidium* sp. and *Uronema*-like abundances remained low (0.04 ± 0.05 × 10³ cells·L⁻¹). In the O treatment, ciliate abundances increased by a factor of 5, i.e. less than in the natural environment. Their size structure changed over the course of the experiment. Like in the control (C) treatment, tintinnids were no longer detected from day 6 on. At the beginning, small ciliates (12.5 to 25 μm) dominated the community with a marked increase in abundances on day 9. At the time of the last count, abundances were 1.20 ± 0.08 × 10³ cells·L⁻¹ and Urotrich and *Uronema*-like dominated the community.

3.7. Principal component analysis (PCA)

PCA analysis was performed on 16 variables (Temp, O_2, NID, PO_4^{3-}, $Si(OH)_4$, ΣH_2S, Viruses, H.Prokaryotes, CYANO, PEUK, NANO, Chl*a*.Ultra, Chl*a*.Nano, Chl*a*.Micro, Chl*b* and Chl*c*). The first axis explained 55.77% of the total inertia of the dataset and the second axis 20.15%, corresponding to a total of 75.92% (Fig. 9). The first axis was negatively correlated with oxygen and positively correlated with DIN, Chl*a*.Ultra, H.Prokaryotes, PO_4^{3-}, ΣH_2S, Chl*b*, PEUK. This axis contrasted the O treatment with high values, from the two other treatments. The second axis was positively correlated with CYANO and to a lesser extent with Temp, Chl*c* and NANO, and negatively correlated with $Si(OH)_4$. On this axis, the high contributions of N and C stand out.

4. Discussion

4.1. Oxygen dynamics and oyster behaviour

In the natural environment (N treatment), the oxygen varied with a nycthemeral dynamic. The higher values were observed during the day because of the oxygen produced by the primary producers. The greater variation in O_2 variation in the Benthic layer, suggest that the benthic compartment (i.e. macrophyte, macroalgae and microphytobenthos) was also a significant driver of O_2 dynamics. The high oxygen concentration allowed oysters to behave normally throughout the experiment. In the control treatment (C), the mesocosms confined the water mass with no oysters present. Although anoxia was not reached, the oxygen concentration decreased over the course of the experiment with lower concentrations observed in the Benthic layer than in the Pelagic layer. These results are in agreement with those reported by Souchu et al., 1998 and Chapelle et al. (2000). Indeed, lower oxygen concentrations were observed at the Benthic than at the surface of water column in the Thau lagoon during the 1994 and 1997 anoxia events. The lower concentrations are linked to the higher oxygen demand at the sediment-water interface, caused by benthic community respiration and mineralisation of organic matter. Higher day-night oxygen variability was observed in the Benthic layer, linked to the photosynthetic activity of primary producers. As the mesocosms were placed on bare sediment, this suggests an important role for microphytobenthos in the oxygen dynamics, both inside the mesocosm and in the natural environment. The respiration of oysters in the O treatment, i.e. with the 'Oyster mesocosm' caused rapid oxygen depletion. However, anoxia took almost twice as long (52–54 h) to occur compared to what we had expected (30*h*), even though we did not include the benthic oxygen demand in our calculations. These results can be explained by the capacity of oysters to adjust their respiration rate to the level of oxygen (Le Moullac et al., 2007). Indeed, at 25 °C, oyster respiration decreases 3 fold (Le Moullac et al., 2007). Coffin et al. (2021) reported that oysters showed remarkable valve closure synchrony when first exposed to anoxia. This behaviour could explain their reduced oxygen respiration when the
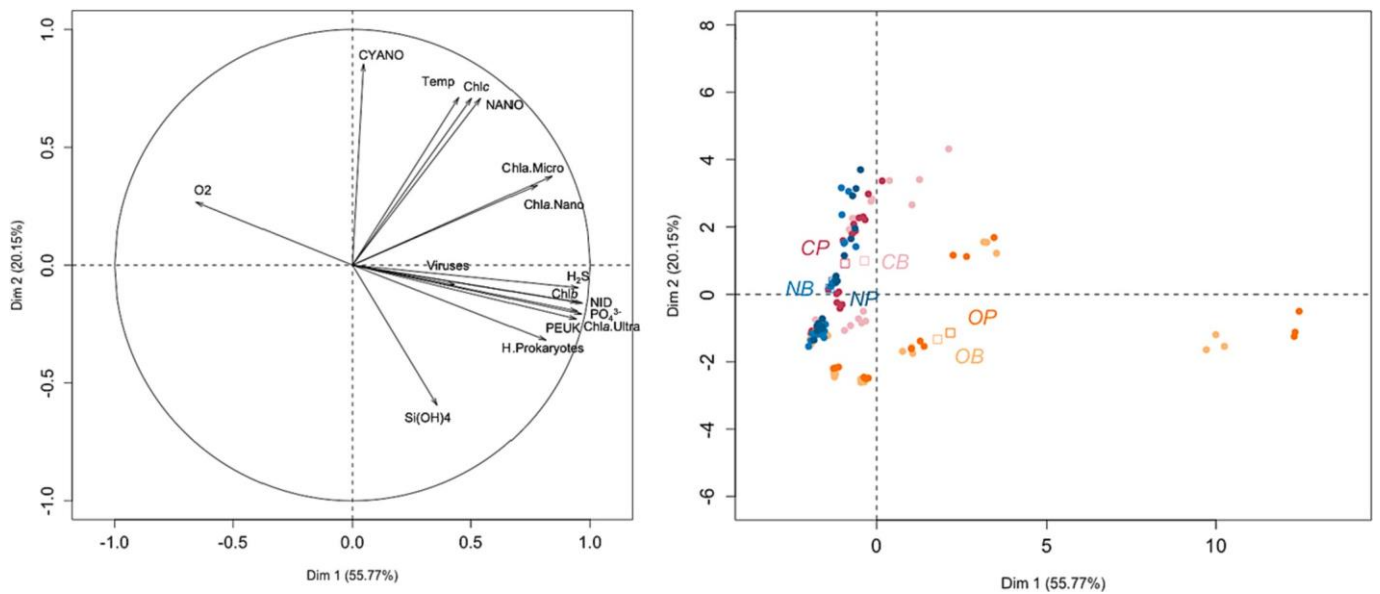
Fig. 9. PCA analysis with 16 variables (Temp, O2, NID, PO43-, Si(OH)4, H2S, Viruses, H.Prokaryotes, CYANO, PEUK, NANO, Chl$a$.Ultra, Chl$a$.Nano, Chl$a$.Micro, Chl$b$ and Chl$c$).

oxygen level is low. According to the observations made by our diver during the experiment, the oysters in the oyster mesocosm (O) were closed on day 2 whereas the oysters reared outside in the natural environment (i.e. in the N treatment) were open. On day 6, the valves of all oysters in the oyster mesocosm were open but some of the oysters reacted to stimuli caused by the scuba diver. On day 9, 100% mortality was observed in the oyster mesocosm, where the valves were open and empty, and some of flesh was seen falling onto the sediment.

4.2. Nutrient dynamics

Confining the water body also had an impact on nutrient concentrations. In the control mesocosm, the mineralisation of organic matter and the reduced oxygen concentration at the sediment-water interface increased the quantity of ammonium and phosphates released from the sediment. However, bacteria abundances did not increase significantly, suggesting that the mineralisation of organic matter was not intense. The measured nutrient concentrations were thus most likely the result of the releases of nutrients from the sediment due to a decrease of oxygen concentrations as already documented worldwide (e.g., Middelburg and Levin, 2009), as well as in the Thau lagoon (Mazouni et al., 1996; Souchu et al., 1998; Dedieu et al., 2007). Very high concentrations of ammonium and phosphates were observed in the oyster mesocosm (treatment O). Indeed, ammonium increases due to the decrease of nitrification (aerobic process) and to increased dissimilatory nitrate reduction to ammonium (DNRA - Mazouni et al., 1996; McCarthy et al., 2008). Phosphates increased close to the sediment and at the sediment-water interface due to the release of iron-bound phosphorus during the reductive dissolution of ferric oxides and hydroxides (Mazouni et al., 1996). These phenomena were already observed in anoxic conditions in the natural environment by Souchu et al. (1998). In addition, decomposition of organic matter (mainly from oyster flesh) from oysters which did not survive the anoxic conditions, strongly enhanced the release of nutrient concentrations (NH_4^+ and PO_4^{3-}). This was already observed during mortality of oyster juveniles in the Thau lagoon in an ex-situ experiment (Richard et al., 2017) when a 6-fold increase in ammonium and a 41-fold increase in phosphates were observed, compared to a respectively 400 and 100-fold increase in the present study. Potential nitrogen and phosphorus release was calculated based on the oyster biomass and analyses of their nitrogen and phosphorus content (data not shown – 8.16% of N and 0.51 of P). Relative to the 270 L of water in the

mesocosm, we estimated the potential release of nitrogen and phosphorous following the decomposition of the oysters (83.7 ± 17.5 g) to be 1108 μmol·L^{-1} of nitrogen and 31.1 μmol·L^{-1} of phosphorus. However, the maximum values obtained (389 μmol·L^{-1} for nitrogen and 17.9 μmol·L^{-1} for phosphorus) were lower than this potential. This may be due to the uptake of nutrients by the phytoplankton and heterotrophic prokaryotes combined with the progressive decomposition of oyster flesh. During the study, silicates were present in significant quantities in the oyster mesocosm (treatment O) and were not limiting, as already observed in the Thau lagoon (Bec et al., 2005). Most of the parameters had decreased on day 13 of the experiment. This decrease in nutrient concentrations (NH_4^+ and PO_4^{3-}) may be due to the end of decomposition of oyster flesh coupled with consumption by phytoplankton.

4.3. Community shift - Bacterial and viral dynamics

In the oyster mesocosm, bacterial abundances increased before oyster mortalities were observed. Oyster mortalities occurred between day 6 and day 9 and are probably due to a combination of several factors: the lack of oxygen, the presence of bacteria and the appearance of sulfides in the water column. In anoxia, SO_4^{2-} are the electron acceptors used for the anaerobic degradation of organic matter that trigger the release of toxic hydrogen sulfide (Pfennig, 1975; Middelburg and Levin, 2009). The synergistic effect of oxygen depletion and the presence of toxic sulfides in oyster mortality has been highlighted by (Vaquer-Sunyer and Duarte, 2010). However, mollusks show a high tolerance to hypoxia/anoxia combined with high hydrogen sulfide values (maximum 279 μmol·L^{-1} - Riedel et al. (2012)), compared to 294 μmol·L^{-1} in the present study when all oysters from the oyster mesocosm had died.

Bacteria were likely the major factor in oyster mortality following oxygen depletion and H2S impairment. Coffin et al. (2021) used antibiotics to control bacterial production under anoxia and it doubled survival time. They showed that proliferation of anaerobic bacteria and/or sulphate-reducing bacteria under anoxic conditions drives oyster mortality (*Crassostrea virginica*). To distinguish between the effect of anaerobic bacteria and sulphate-reducing bacteria, De Zwaan et al. (2002), used molybdate (inhibitor of sulphate-reduction) to block sulfide biotic production and it did not improve clams survival time indicating that sulfide and sulphate-reducing bacteria are not the major cause of mortality. This suggest that the major cause of bivalve mortality in anoxia is induced by the proliferation of pathogenic anaerobic

bacteria, probably causing lesions on bivalve flesh. The bacterial community can therefore be a cause of oyster mortalities, however, these mortalities will also impact the bacterial community itself. At the time of the mortalities, between day 6 and 9, the abundances of heterotrophic prokaryotes increased strongly, associated with the decomposition of the oyster flesh via anaerobic pathways. In the present study, bacterial abundances were multiplied by 16 at day 9 when the shells were seen to be empty following the mortalities (between day 6 and day 9). This proliferation probably inducing the milky colour of the water inside the oyster mesocosm.

Once the flesh was decomposed, these abundances decreased probably associated with a community shift. Souchu et al. (1998) suggested the presence of Chlorobiaceae and Chromatiaceae in the Thau lagoon during anoxia. These bacteria could be involved in the re-oxidation of sulphides by anoxygenic phototrophic bacteria (Pfennig, 1975; Barton et al., 2014). This would explain the decrease in hydrogen sulphide concentrations on day 13 of the experiment. Metabarcoding analyses are considered to analyse the bacterial diversity to confirm the presence of species linked to the sulfur cycle and species associated with massive oyster mortality event (De Lorgeril et al., 2019; Richard et al., 2022).

Kan et al. (2006) demonstrated a correlation between bacterial and viral abundances in Chesapeake Bay. In the same way, in our study, viral abundances increased during oyster mortality and continued to increase until the end of the experiment. In the O treatment, oysters could be a potential reservoir of virus as previously seen in the case of herpesvirus (Arzul et al., 2002).

4.4. Community shift - Phytoplankton dynamics

In the natural environment (treatment N), the change in the biological parameters was linked to the water temperature which increased to 25.3 °C. This slightly enhanced the growth of phytoplanktonic communities, particularly microphytoplankton, autotrophic flagellates and cyanobacteria. Values of chl$a$ biomass (0.58 to 0.98 µg·L^{-1}) were similar to those recorded previously (0.62 µg·L^{-1} in September 1999 – Bec et al., 2005). In the control mesocosm (treatment C), the phytoplankton biomass increased over time more than in the natural environment (treatment N). This increase in the phytoplankton biomass occurred in the Benthic layer due to the release of nutrients at the water-sediment interface. The increase was attributed to microphytoplankton associated with golden brown algae. Heterotrophic flagellate abundances also increased but less than in the natural environment (treatment N). This could be explained by the fact that they are predators of bacteria and organic matter (Gonzalez et al., 1990), which were not as abundant as in the N treatment. Ciliate abundances increased and then decreased with the disappearance of loricate ciliates (tintinnids), which probably suffered from the low oxygen concentrations. This observation on tintinnids has already been observed in situ in Chesapeake Bay, where they are no longer detectable under 2 mg·L^{-1} of oxygen (Dolan and Coats, 1991). The conditions in the C mesocosm also had an impact on the trophic chain with the removal of the top-down control of filter feeders (Dupuy et al., 2000) originally present at this rearing site, which favour phytoplankton and protist predators. In contrast to the natural environment (treatment N) and in the control mesocosm (treatment C), in the oyster mesocosm (treatment O) the ultraphytoplankton bloom associated with green algae (< 5 µm) was observed after oyster mortality, on day 9. A bloom associated with small green algae has also been reported during a previous mortality event of oyster juveniles in the Thau lagoon (Richard et al., 2019). In the present study, ultraphytoplankton was dominated by a single population of picoeukaryotes, around 3–4 µm in size, reminiscent of the green water phenomenon reported in 2018, in which one species of Picochlorum sp. dominated the phytoplankton community of the lagoon (Lagarde et al., 2021). Metabarcoding analyses are considered to confirm or infirm the presence of this chlorophyte. Picophytoplankton abundances in the anoxic oyster mesocosm (mean at both depths: 186 × 10^6 cells·L^{-1}) resembled the

high abundances already observed in the Thau lagoon in the summer of 1993: 180 × 10^6 cells·L^{-1} (Vaquer et al., 1996). However, they remained very high compared to the annual average of 35 × 10^6 cells·L^{-1}, with a maximum in April of 90.8 × 10^6 cells·L^{-1} measured in 1999 by Bec et al. (2005). The dominance of small green algae is influenced by several parameters, but particularly by the available source of nutrients and the ability of this phytoplankton to live in an anoxic and sulphidic environment. Nutrient availability and the source of nutrients are major factors influencing the community structure of phytoplankton in coastal lagoons (Bec et al., 2011). Small phytoplankton are known to accomplish the majority of regenerated production from ammonium (Glibert et al., 1991; Collos et al., 2003; Bec et al., 2011). Regenerated production from ammonium was favoured during our experiments in which DIN is composed of 99% of ammonium. Amongst this phytoplankton, only species capable of withstanding anoxia and the possibly toxic high concentrations of H_2S and NH_4 will be able to grow. Green algae have the enzymes that allow them to switch to anaerobic metabolism, like mixed-acid fermentation (Atteia et al., 2013). High concentrations of acetate were measured in the oyster mesocosm (treatment O) during the experiment (data not shown), which can be used for anaerobic metabolism. This phytoplanktonic community shift was induced by the presence of oysters. On one hand, ultra-phytoplankton was not consumed by the oysters as their size (< 5 µm) is below that which adult oyster filters can retain (Dupuy et al., 2000), and oysters were already dead on the day of the bloom, while, on the other hand, ultraphytoplankton is controlled by grazing protists (Bec et al., 2005). Also, Cylindrotheca spp. were found on the walls of the mesocosm, perhaps linked to the post-anoxia diatom blooms observed in situ (Lagarde et al., 2021; Philippe Souchu et al., 1998). Autotrophic flagellates were no longer detected in the oyster mesocosm (treatment O). These flagellates had probably already been filtered out by the oysters or predated by ciliates (Mostajir et al., 2015a; Richard et al., 2019), but they may also be less resistant to anoxia. Heterotrophic prokaryotes were particularly abundant in the oyster mesocosm (107 × 10^6 cells·L^{-1}) and were about 70 times more abundant than those observed in a previous mesocosm experiment with living oysters (Mostajir et al., 2015b). Small heterotrophic flagellates (< 5 µm), known to feed on bacteria-sized particles (Fenchel, 1982), and themselves poorly filtered by oysters (Dupuy et al., 2000), increased significantly in the oyster mesocosm over the course of the experiment. Heterotrophic flagellates are an essential link between bacteria and the larger organisms in the microbial food web (Fenchel, 1982; Bec et al., 2005; Mostajir et al., 2015a). The abundances of naked ciliates increased in anoxia, linked to the abundance of their food sources, bacteria, flagellates, picophytoplankton and nanophytoplankton (Rassoulzadegan et al., 1988), in the oyster mesocosm (treatment O). An increase in the abundance of naked ciliates has already been reported during mortalities of oyster juveniles when Strombilidium sp., Uronema sp., Balanion sp. and Strombidium sp. dominated the community (Richard et al., 2019). Tintinnids did not survive the anoxic conditions in the oyster mesocosm, as they are very sensitive to the concentration of oxygen and do not tolerate oxygen deficits (Dolan and Coats, 1991). Even if the living conditions were not ideal during anoxia, some ciliates tolerated anoxia and developed in this condition. Two hypotheses have been put forward to explain this tolerance to anoxia: (1) a symbiosis between a ciliate (mostly Euplotes sp, present in the O mesocosm) with an alga of the type Chlorella spp. (Finlay et al., 1996), (2) the presence of micro-aerobic ciliates (like Euplotes sp., Uronema sp. and Strombidium sp.), whose optimal oxygen window is between 1% and 20% saturation and which can maintain metabolic activity in anoxia with high H_2S concentrations (Bernard and Fenchel, 1996). As this symbiosis has been observed in freshwater and for strict anaerobic ciliates (Fenchel and Finlay, 1991), in the present study, the second hypothesis is more likely. Dubber and Gray (2011) showed that the longer anoxia continues, the bigger the reduction in species richness and in the total abundances of ciliates. The same authors also noted that ciliate abundances were able to increase over time

when tolerant species were established, as was the case in the present study. However, their growth rates remain limited by the anoxic conditions (Bernard and Fenchel, 1996). The changes in microbial plankton structure we observed are similar to those observed in oyster juvenile mortalities by Richard et al. (2019). At the end of the experiment (day 13), due to unfavourable conditions combining anoxia and sulfur toxicity, the abundances of most of the microbial components had decreased due to their sensitivity to these conditions.

4.5. Conclusion and perspectives

The in-situ study allowed for the first time to artificially reproduce an anoxia phenomenon in the natural environment. In a closed system, the respiration of oysters coupled to the benthic oxygen demand have induced an anoxia in 54 h. Anoxia and oyster mortality caused an increase of up to 390 $\mu mol \cdot L^{-1}$ in inorganic dissolved nitrogen (dominated by ammonium) and up to 17 $\mu mol \cdot L^{-1}$ in phosphates, through the decomposition of oyster flesh and releases from the sediment-water interface. These high inputs increased phytoplankton biomass by 20 fold (11.8 μg chl$a \cdot L^{-1}$) and their abundances by 4 fold (186 $\times$ 10^6 cells$\cdot L^{-1}$) associated with one population of green algae (3–4 μm). In these conditions, protist grazers (heterotrophic flagellates and ciliates) were able to develop. Also, some large ciliate species were observed at the end of the experiment, although their abundances were twice lower than in the natural environment (treatment N). Oyster mortality had a major influence during the anoxic crisis in oligotrophic waters, favouring blooms of small microbial planktonic components following a notable release of nutrients due to the decomposition of oyster flesh and nutrient releases at the water-sediment interface. A community shift towards a trophic web made of smaller species was observed as consequences of oyster mortality. In the Thau lagoon, such a shift would not support shellfish farming, and could have an impact on oyster growth as was the case in 2018 (Richard et al., 2022). The use of mesocosms allowed us to reproduce and measure the effects of an anoxia event in the Thau lagoon like the event observed in 2018. The consequences of the oxygen deficit are therefore a real problem facing the Thau lagoon. High-frequency monitoring of oxygen levels would deepen our understanding of oxygen dynamics in the Thau lagoon and help predict anoxia events, by monitoring early hypoxia during the night. Until then, preventive measures could be taken: avoid shallow zones to rear oysters, take oysters out of the water during the night using a mechanical system to mimic low tide and reduce oxygen demand by the ecosystem. If anoxia occurs, removing shellfish before mortality and decomposition occur would limit nutrient enrichment, and reduce the probability of virus, bacteria and picophytoplankton development to the detriment of diatom blooms, as well as reduce the ecological impact on the pelagic community.

CRediT authorship contribution statement

Julie Le Ray: Formal analysis, Investigation, Data curation, Writing – original draft, Writing – review & editing, Visualization. **Béatrice Bec:** Conceptualization, Investigation, Resources, Writing – review & editing, Supervision, Funding acquisition. **Annie Fiandrino:** Conceptualization, Writing – review & editing, Supervision, Funding acquisition. **Franck Lagarde:** Investigation, Writing – review & editing. **Nicolas Cimiterra:** Investigation, Resources, Writing – review & editing. **Patrick Raimbault:** Investigation, Resources. **Cécile Roques:** Investigation, Resources. **Sylvain Rigaud:** Investigation, Resources, Writing – review & editing. **Julie Régis:** Investigation, Resources. **Behzad Mostajir:** Investigation, Writing – review & editing. **Sébastien Mas:** Resources. **Marion Richard:** Conceptualization, Methodology, Investigation, Resources, Writing – review & editing, Supervision, Project administration, Funding acquisition.

Declaration of Competing Interest

The authors declare that they have no known competing financial interests or personal relationships that could have appeared to influence the work reported in this paper.

Data availability

Data will be made available on request.

Acknowledgements

Appendix A. Supplementary data

Supplementary data to this article can be found online at https://doi.org/10.1016/j.aquaculture.2022.739171.

References

Aminot, A., Kérouel, R., Quae, 2007. Dosage automatique des nutriments dans les eaux marines : méthodes en flux continu, p. 188.

Antoniades, D., Michelutti, N., Quinlan, R., Blais, J.M., Bonilla, S., Douglas, M.S.V., Pienitz, R., Smol, J.P., Vincent, W.F., 2011. Cultural eutrophication, anoxia, and ecosystem recovery in Meretta Lake, high Arctic Canada. Limnol. Oceanogr. 56, 639–650. https://doi.org/10.4319/lo.2011.56.2.0639.

Arzul, I., Renault, T., Thébault, A., Gérard, A., 2002. Detection of oyster herpesvirus DNA and proteins in asymptomatic *Crassostrea gigas* adults. Virus Res. 84, 151–160. https://doi.org/10.1016/S0168-1702(02)00007-2.

Atteia, A., van Lis, R., Tielens, A.G.M., Martin, W.F., 2013. Anaerobic energy metabolism in unicellular photosynthetic eukaryotes. Biochim. Biophys. Acta - Bioenerg. 1827, 210–223. https://doi.org/10.1016/j.bbabio.2012.08.002. The evolutionary aspects of bioenergetic systems.

Balzer, W., Grasshoff, K., Dieckmann, P., Haardt, H., Petersohn, U., 1983. Redox-turnover at the sediment/water interface studied in a large bell jar system. Oceanol. Acta 6.

Barton, L.L., Fardeau, M.-L., Fauque, G.D., 2014. Hydrogen sulfide: A toxic gas produced by dissimilatory sulfate and sulfur reduction and consumed by microbial oxidation. In: Kroneck, P.M.H., Torres, M.E.S. (Eds.), The Metal-Driven Biogeochemistry of Gaseous Compounds in the Environment, Metal Ions in Life Sciences. Springer, Netherlands, Dordrecht, pp. 237–277. https://doi.org/10.1007/978-94-017-9269-1_10.

Bec, B., Husseini-Ratrema, J., Collos, Y., Souchu, P., Vaquer, A., 2005. Phytoplankton seasonal dynamics in a Mediterranean coastal lagoon: emphasis on the picoeukaryote community. J. Plankton Res. 27, 881–894. https://doi.org/10.1093/plankt/fbi061.

Bec, B., Collos, Y., Souchu, P., Vaquer, A., Lautier, J., Fiandrino, A., Benau, L., Orsoni, V., Laugier, T., 2011. Distribution of picophytoplankton and nanophytoplankton along an anthropogenic eutrophication gradient in French Mediterranean coastal lagoons. Aquat. Microb. Ecol. 63, 29–45. https://doi.org/10.3354/ame01480.

Bernard, C., Fenchel, T., 1996. Some microaerobic ciliates are facultative anaerobes. Eur. J. Protistol. 32, 293–297. https://doi.org/10.1016/S0932-4739(96)80051-4.

Boynton, W.R., Murray, L., Hagy, J.D., Stokes, C., Kemp, W.M., 1996. A comparative analysis of eutrophication patterns in a temperate coastal lagoon. Estuaries 19, 408–421. https://doi.org/10.2307/1352459.

Breitburg, D., Levin, L.A., Oschlies, A., Grégoire, M., Chavez, F.P., Conley, D.J., Garçon, V., Gilbert, D., Gutiérrez, D., Isensee, K., Jacinto, G.S., Limburg, K.E., Montes, I., Naqvi, S.W.A., Pitcher, G.C., Rabalais, N.N., Roman, M.R., Rose, K.A., Seibel, B.A., Telszewski, M., Yasuhara, M., Zhang, J., 2018. Declining oxygen in the global ocean and coastal waters. Science 359. https://doi.org/10.1126/science.aam7240.

Brussaard, C.P.D., 2004. Optimization of procedures for counting viruses by flow cytometry. Appl. Environ. Microbiol. 70, 1506–1513. https://doi.org/10.1128/AEM.70.3.1506-1513.2004.

Chapelle, A., Ménesguen, A., Deslous-Paoli, J.-M., Souchu, P., Mazouni, N., Vaquer, A., Millet, B., 2000. Modelling nitrogen, primary production and oxygen in a

Mediterranean lagoon. Impact of oysters farming and inputs from the watershed. Ecol. Model. 127, 161–181. https://doi.org/10.1016/S0304-3800(99)00206-9.

Cline, J., 1969. Spectrophotometric determination of hydrogen sulfide in natural waters. Limnol. Oceanogr. 14, 454–458.

Coffin, M.R.S., Clements, J.C., Comeau, L.A., Guyondet, T., Maillet, M., Steeves, L., Winterburn, K., Babarro, J.M.F., Mallet, M.A., Hach´e, R., Poirier, L.A., Deb, S., Filgueira, R., 2021. The killer within: endogenous bacteria accelerate oyster mortality during sustained anoxia. Limnol. Oceanogr. 66, 2885–2900. https://doi.org/10.1002/lno.11798.

Collos, Y., Vaquer, A., Bibent, B., Souchu, P., Slawyk, G., Garcia, N., 2003. Response of coastal phytoplankton to ammonium and nitrate pulses: seasonal variations of nitrogen uptake and regeneration. Aquat. Ecol. 37, 227–236. https://doi.org/10.1023/A:1025881323812.

D'Avanzo, C., Kremer, J.N., 1994. Diel oxygen dynamics and anoxic events in an eutrophic estuary of Waquoit Bay, Massachusetts. Estuaries 17, 131–139. https://doi.org/10.2307/1352562.

De Lorgeril, M., Salen, P., Rabaeus, M., 2019. New and traditional foods in a modernized Mediterranean diet model. Eur. J. Clin. Nutr. 72 (1), 47–54. https://doi.org/10.1038/s41430-018-0308-6.

De Zwaan, A., Babarro, J.M.F., Monari, M., Cattani, O., 2002. Anoxic survival potential of bivalves: (arte)facts. Comp. Biochem. Physiol. Part A - Mol. Integr. Physiol. 131A (3), 615–624.

Dedieu, K., Rabouille, C., Gilbert, F., Soetaert, K., Metzger, E., Simonucci, C., J´ez´equel, D., Pr´evot, F., Anschutz, P., Hulth, S., Ogier, S., Mesnage, V., 2007. Coupling of carbon, nitrogen and oxygen cycles in sediments from a Mediterranean lagoon: a seasonal perspective. Mar. Ecol. Prog. Ser. 346, 45–59. https://doi.org/10.3354/meps07031.

Derolez, V., Malet, N., Fiandrino, A., Lagarde, F., Richard, M., Ouisse, V., Bec, B., Aliaume, C., 2020a. Fifty years of ecological changes: regime shifts and drivers in a coastal Mediterranean lagoon during oligotrophication. Sci. Total Environ. 732, 139292 https://doi.org/10.1016/j.scitotenv.2020.139292.

Derolez, V., Soudant, D., Malet, N., Chiantella, C., Richard, M., Abadie, E., Aliaume, C., Bec, B., 2020b. Two decades of oligotrophication: evidence for a phytoplankton community shift in the coastal lagoon of Thau (Mediterranean Sea, France). Estuar. Coast. Shelf Sci. 241, 106810 https://doi.org/10.1016/j.ecss.2020.106810.

Diaz, R.J., Rosenberg, R., 2008. Spreading dead zones and consequences for marine ecosystems. Science 321, 926–929. https://doi.org/10.1126/science.1156401.

Dolan, J., Coats, D., 1991. Changes in fine-scale vertical distribution of ciliate micro-zooplankton related to anoxia in Chesapeake Bay waters. Mar. Microb. Food Webs 5, 81–93.

Dubber, D., Gray, N.F., 2011. The effect of anoxia and anaerobia on ciliate community in biological nutrient removal systems using laboratory-scale sequencing batch reactors (SBRs). Water Res. 45, 2213–2226. https://doi.org/10.1016/j.watres.2011.01.015.

Dupuy, C., Vaquer, A., Lam-Ho¨ai, T., Rougier, C., Mazouni, N., Lautier, J., Collos, Y., Le Gall, S., 2000. Feeding rate of the oyster Crassostrea gigas in a natural planktonic community of the Mediterranean Thau Lagoon. Mar. Ecol. Prog. Ser. 205, 171–184. https://doi.org/10.3354/meps205171.

Fenchel, T., 1982. Ecology of heterotrophic microflagellates. I. Some important forms and their functional morphology. Mar. Ecol. Prog. Ser. 8, 211–223.

Fenchel, T., Finlay, B.J., 1991. The biology of free-living anaerobic ciliates. Eur. J. Protistol. 26, 201–215. https://doi.org/10.1016/S0932-4739(11)80143-4.

Fiandrino, A., Ouisse, V., Dumas, F., Lagarde, F., Pete, R., Malet, N., Le Noc, S., de Wit, R., 2017. Spatial patterns in coastal lagoons related to the hydrodynamics of seawater intrusion. Mar. Pollut. Bull. 119, 132–144. https://doi.org/10.1016/j.marpolbul.2017.03.006.

Finlay, B.J., Maberly, S.C., Esteban, G.F., 1996. Spectacular abundance of ciliates in anoxic pond water: contribution of symbiont photosynthesis to host respiratory oxygen requirements. FEMS Microbiol. Ecol. 20, 229–235. https://doi.org/10.1111/j.1574-6941.1996.tb00321.x.

Gangnery, A., Bacher, C., Buestel, D., 2001. Assessing the production and the impact of cultivated oysters in the Thau lagoon (Mediterran´ee, France) with a population dynamics model. Can. J. Fish. Aquat. Sci. 58, 1012–1020. https://doi.org/10.1139/f01-028.

Gangnery, A., Chabirand, J.-M., Lagarde, F., Le Gall, P., Oheix, J., Bacher, C., Buestel, D., 2003. Growth model of the Pacific oyster, Crassostrea gigas, cultured in Thau Lagoon (M´editerran´ee, France). Aquaculture 215, 267–290. https://doi.org/10.1016/S0044-8486(02)00351-4.

Glibert, P.M., Garside, C., Fuhrman, J.A., Roman, M.R., 1991. Dependent coupling of inorganic and organic nitrogen uptake and regeneration in the plume of the Chesapeake Bay estuary and its regulation by large heterotrophs. Limnol. Oceanogr. 36, 895–909. https://doi.org/10.4319/lo.1991.36.5.0895.

Gonzalez, J.M., Sherr, E.B., Sherr, B.F., 1990. Size-selective grazing on bacteria by natural assemblages of estuarine flagellates and ciliates. Appl. Environ. Microbiol. 56, 583–589. https://doi.org/10.1128/aem.56.3.583-589.1990.

Gooday, A.J., Jorissen, F., Levin, L.A., Middelburg, J.J., Naqvi, S.W.A., Rabalais, N.N., Scranton, M., Zhang, J., 2009. Historical records of coastal eutrophication-induced hypoxia. Biogeosciences 6, 1707–1745. https://doi.org/10.5194/bg-6-1707-2009.

Guelorget, O., Perthuisot, J., Lamy, N., Lefebvre, A., 1994. Structure et organisation de l´´etang de Thau d'apr`es la faune benthique (macrofaune, m´eiofaune). Relations avec le confinement. Oceanol. Acta 17, 105–114.

Hamon, P.-Y., Vercelli, C., Pichot, Y., Lagarde, F., Le Gall, P., Oheix, J., 2003. Les malaïgues de l´´etang de Thau. Tome 1 (Description des malaïgues. Moyens de lutte, recommandations).

Harzallah, A., Chapelle, A., 2002. Contribution of climate variability to occurrences of anoxic crises 'malaïgues' in the Thau lagoon (southern France). Oceanol. Acta 25, 79–86. https://doi.org/10.1016/S0399-1784(02)01184-2.

Holmes, R.M., Aminot, A., K´erouel, R., Hooker, B.A., Peterson, B.J., 1999. A simple and precise method for measuring ammonium in marine and freshwater ecosystems. Can. J. Fish. Aquat. Sci. 56, 1801–1808. https://doi.org/10.1139/f99-128.

Kan, J., Crump, B.C., Wang, K., Chen, F., 2006. Bacterioplankton community in Chesapeake Bay: predictable or random assemblages. Limnol. Oceanogr. 51, 2157–2169. https://doi.org/10.4319/lo.2006.51.5.2157.

Lagarde, F., Bec, B., Atteia Van Lis, A., Gobet, A., Richard, M., Derolez, V., Mostajir, B., Roques, C., Foucault, E., Messiaen, G., Hubert, C., Cimiterra, N., 2021. Ph´enom`ene d'Eaux Vertes a` Picochlorum en lagune de Thau pendant les ann´ees 2018 et 2019. Ifremer, Observations environnementales. https://doi.org/10.13155/80087.

Le Moullac, G., Qu´eau, I., Le Souchu, P., Pouvreau, S., Moal, J., Rene´ Le Coz, J., François Samain, J., 2007. Metabolic adjustments in the oyster Crassostrea gigas according to oxygen level and temperature. Mar. Biol. Res. 3, 357–366. https://doi.org/10.1080/17451000701635128.

Lomstein, B.A., Guldberg, L.B., Hansen, J., 2006. Decomposition of Mytilus edulis: the effect on sediment nitrogen and carbon cycling. J. Exp. Mar. Biol. Ecol. 329, 251–264. https://doi.org/10.1016/j.jembe.2005.09.003.

Marie, D., Partensky, F., Jacquet, S., Vaulot, D., 1997. Enumeration and cell cycle analysis of natural populations of marine picoplankton by flow cytometry using the nucleic acid stain SYBR green I. Appl. Environ. Microbiol. 63, 186–193. https://doi.org/10.1128/aem.63.1.186-193.1997.

Mazouni, N., Gaertner, J.-C., Deslous-Paoli, J.-M., Landrein, S., Geringer d'Oedenberg, M., 1996. Nutrient and oxygen exchanges at the water–sediment interface in a shellfish farming lagoon (Thau, France). J. Exp. Mar. Biol. Ecol. 205, 91–113. https://doi.org/10.1016/S0022-0981(96)02594-4.

McCarthy, M.J., McNeal, K.S., Morse, J.W., Gardner, W.S., 2008. Bottom-water Hypoxia Effects on Sediment–Water Interface Nitrogen Transformations in a Seasonally Hypoxic, Shallow Bay (Corpus Christi Bay, TX, USA). Estuar. Coasts 31, 521–531. https://doi.org/10.1007/s12237-008-9041-z.

Middelburg, J.J., Levin, L.A., 2009. Coastal Hypoxia and Sediment Biogeochemistry 21.

Mostajir, B., Amblard, C., Buffan-Dubau, E., De Wit, R., Lensi, R., Sime-Ngando, T., 2015a. Microbial food webs in aquatic and terrestrial ecosystems. In: Bertrand, J.-C., Caumette, P., Lebaron, P., Matheron, R., Normand, P., Sime-Ngando, T. (Eds.), Environmental Microbiology: Fundamentals and Applications: Microbial Ecology. Springer, Netherlands, Dordrecht, pp. 485–509. https://doi.org/10.1007/978-94-017-9118-2_13.

Mostajir, B., Roques, C., Bouvier, C., Bouvier, T., Fouilland, E´., Got, P., Floc'h, E.L., Nouguier, J., Mas, S., Semp´er´e, R., Sime-Ngando, T., Troussellier, M., Vidussi, F., 2015b. Microbial food web structural and functional responses to oyster and fish as top predators. Mar. Ecol. Prog. Ser. 535, 11–27. https://doi.org/10.3354/meps11429.

Neveux, J., Lantoine, F., 1993. Spectrofluorometric assay of chlorophylls and phaeopigments using the least squares approximation technique. Deep-Sea Res. I Oceanogr. Res. Pap. 40, 1747–1765. https://doi.org/10.1016/0967-0637(93)90030-7.

Newton, A., Icely, J.D., Falcao, M., Nobre, A., Nunes, J.P., Ferreira, J.G., Vale, C., 2003. Evaluation of eutrophication in the ria Formosa coastal lagoon, Portugal. Continental Shelf Research. Eu. Land-Ocean Interact. 23, 1945–1961. https://doi.org/10.1016/j.csr.2003.06.008.

Pack, K.E., Rius, M., Mieszkowska, N., 2021. Long-term environmental tolerance of the non-indigenous Pacific oyster to expected contemporary climate change conditions. Mar. Environ. Res. 164, 105226 https://doi.org/10.1016/j.marenvres.2020.105226.

Pernet, F., Tremblay, R., Comeau, L., Guderley, H., 2007. Temperature adaptation in two bivalve species from different thermal habitats: energetics and remodelling of membrane lipids. J. Exp. Biol. 210, 2999–3014. https://doi.org/10.1242/jeb.006007.

Pfennig, N., 1975. The phototrophic bacteria and their role in the sulfur cycle. Plant Soil 43, 1–16. https://doi.org/10.1007/BF01928472.

Po¨rtner, H., 2001. Climate change and temperature-dependent biogeography: oxygen limitation of thermal tolerance in animals. Naturwissenschaften 88, 137–146. https://doi.org/10.1007/s001140100216.

Rassoulzadegan, F., Laval-Peuto, M., Sheldon, R.W., 1988. Partitioning of the food ration of marine ciliates between pico- and nanoplankton. Hydrobiologia 159, 75–88. https://doi.org/10.1007/BF00007369.

Richard, M., Bourreau, J., Montagnani, C., Ouisse, V., Le Gall, P., Fortune, M., Munaron, D., Messiaen, G., Callier, M.D., Roque d'Orbcastel, E., 2017. Influence of OSHV-1 oyster mortality episode on dissolved inorganic fluxes: an ex situ experiment at the individual scale. Aquaculture 475, 40–51. https://doi.org/10.1016/j.aquaculture.2017.03.026.

Richard, M., Bec, B., Vanhuysse, C., Mas, S., Parin, D., Chantalat, C., Le Gall, P., Fiandrino, A., Lagarde, F., Mortreux, S., Ouisse, V., Rolland, J.L., Degut, A., Hatey, E., Fortune, M., Roque d'Orbcastel, E., Messiaen, G., Munaron, D., Callier, M., Oheix, J., Derolez, V., Mostajir, B., 2019. Changes in planktonic microbial components in interaction with juvenile oysters during a mortality episode in the Thau lagoon (France). Aquaculture 503, 231–241. https://doi.org/10.1016/j.aquaculture.2018.12.082.

Richard, M., Bec, B., Bergeon, L., H´ebert, M., Mablouk´e, C., Lagarde, F., 2022. Are mussels and oysters capable of reducing the abundances of Picochlorum sp., responsible for a massive green algae bloom in Thau lagoon, France? J. Exp. Mar. Biol. Ecol. 556, 151797 https://doi.org/10.1016/j.jembe.2022.151797.

Riedel, B., Zuschin, M., Stachowitsch, M., 2012. Tolerance of benthic macrofauna to hypoxia and anoxia in shallow coastal seas: a realistic scenario. Mar. Ecol. Prog. Ser. 458, 39–52. https://doi.org/10.3354/meps09724.

Schmidtko, S., Stramma, L., Visbeck, M., 2017. Decline in global oceanic oxygen content during the past five decades. Nature 542, 335–339. https://doi.org/10.1038/nature21399.

Souchu, Philippe, Gasc, A., Collos, Y., Vaquer, A., Tournier, H., Bibent, B., Deslous-Paoli, J.-M., 1998. Biogeochemical aspects of bottom anoxia in a Mediterranean lagoon (Thau, France). Mar. Ecol. Prog. Ser. 164, 135–146. https://doi.org/10.3354/meps164135.

Souchu, P., Vaquer, A., Collos, Y., Landrein, S., Deslous-Paoli, J., Bibent, B., 2001. Influence of shellfish farming activities on the biogeochemical composition of the water column in Thau lagoon. Mar. Ecol. Prog. Ser. 218, 141–152. https://doi.org/10.3354/meps218141.

Utermö̈hl, H., 1958. Methods of collecting plankton for various purposes are discussed. SIL Commun. 1953-1996 (9), 1–38. https://doi.org/10.1080/05384680.1958.11904091.

van der Loeff, M.M.R., Anderson, L.G., Hall, P.O.J., Iverfeldt, Å., Josefson, A.B., Sundby, B., Westerlund, S.F.G., 1984. The asphyxiation technique: an approach to distinguishing between molecular diffusion and biologically mediated transport at the sediment—water interface. Limnol. Oceanogr. 29, 675–686. https://doi.org/10.4319/lo.1984.29.4.0675.

Vaquer, A., Troussellier, M., Courties, C., Bibent, B., 1996. Standing stock and dynamics of picophytoplankton in the Thau Lagoon (Northwest Mediterranean coast). Limnol. Oceanogr. 41, 1821–1828. https://doi.org/10.4319/lo.1996.41.8.1821.

Vaquer-Sunyer, R., Duarte, C.M., 2010. Sulfide exposure accelerates hypoxia-driven mortality. Limnol. Oceanogr. 55, 1075–1082. https://doi.org/10.4319/lo.2010.55.3.1075.

Vidussi, F., Mostajir, B., Fouilland, E., Floc'h, E.L., Nouguier, J., Roques, C., Got, P., Thibault-Botha, D., Bouvier, T., Troussellier, M., 2011. Effects of experimental warming and increased ultraviolet B radiation on the Mediterranean plankton food web. Limnol. Oceanogr. 56, 206–218. https://doi.org/10.4319/lo.2011.56.1.0206.

Zimmerman, A.R., Canuel, E.A., 2000. A geochemical record of eutrophication and anoxia in Chesapeake Bay sediments: anthropogenic influence on organic matter composition. Mar. Chem. 69, 117–137. https://doi.org/10.1016/S0304-4203(99)00100-0.